Resonant Heating Due to Cyclotron Subharmonic Frequency Waves

H. Abe, H. Okada, and R. Itatani
Department of Electronics, Kyoto University, Kyoto 606, Japan

and

M. Ono and H. Okuda
Plasma Physics Laboratory, Princeton University, Princeton, New Jersey 08544
(Received 18 April 1984)

A direct ion heating process which is resonant with the wave at the cyclotron subharmonic frequency, $\omega = \frac{3}{2}\Omega_i$, is discovered through the particle-simulation investigation of the ion Bernstein-wave heating. The particle trapping in phase space due to the wave of an arbitrary cyclotron subharmonic frequency is studied theoretically and numerically confirmed.

PACS numbers: 52.50.Gj, 52.35.Fp, 52.65.+z

Recently, plasma heating by an externally launched ion Bernstein wave (IBW) has been actively pursued as a promising candidate for heating reactor plasmas to ignition temperatures. In particular, several experiments have yielded very efficient bulk hydrogen-ion heating by utilization of this heating technique.[1,2] We believe the high-efficiency ion-heating results warrant a further investigation of the detailed absorption physics of ion Bernstein waves using the self-consistent particle simulation technique. In this Letter we report, for the first time, existence of a new mechanism for ion heating which occurs at the cyclotron subharmonic resonance, $\omega = \frac{3}{2}\Omega_i$. To understand the simulation results, a theoretical model based on the trapping in phase space is constructed whose validity is then confirmed by single-particle simulation calculations.

The simulation results are improved further by use of a larger simulation system compared with that of Nakajimi, Abe, and Itatani,[3] involving a higher-order spatial interpolation. The ion Bernstein wave is excited by the single mode antenna near the left wall at $\omega = 1.9\Omega_H$ in a hydrogen plasma (H). The ambient magnetic field increases with x so that the wave encounters the $\omega = \frac{3}{2}\Omega_H$ resonance near $x = 100$ (Fig. 1). In this simulation, however, most of the wave energy passes through this region, because the system size is still not large enough for complete absorption by the present mechanism, as shown later. Therefore, we have placed the fundamental cyclotron damping layer in front of the right wall to absorb the wave, and thus eliminated the wave reflection, which greatly simplifies the wave physics.

In Fig. 1(a), the wave potential contours are shown. The corresponding perpendicular-wave electric field is shown in Fig. 1(b). The measured wave number $k_\perp$ is shown as circles in Fig. 1(c). The measured value is in good agreement with the

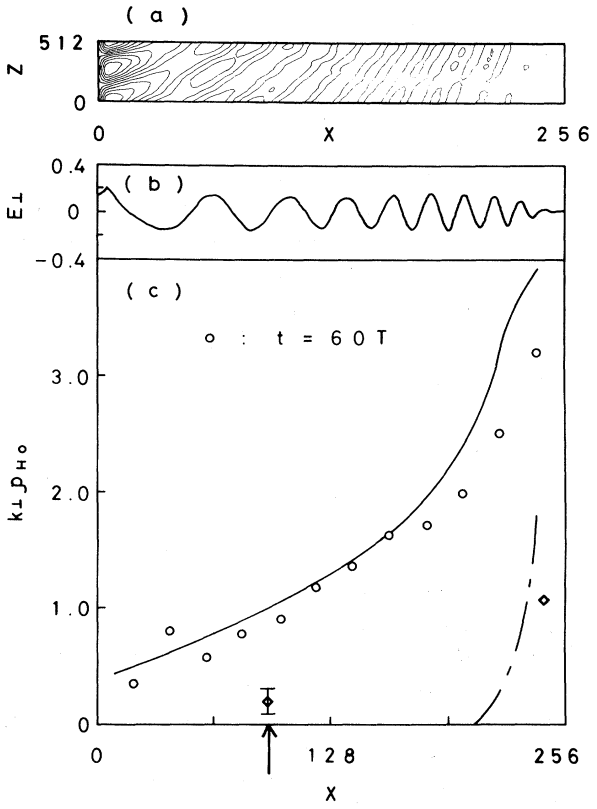

FIG. 1. The wave propagation profiles: (a) Wave potential contours. Distance in the z direction is scaled down by one sixteenth compared with that in the x direction. (b) $E_\perp$ vs x in steady state at $t = 60T$: (c) $k_\perp$ vs x. The solid line and dashed line are the real and imaginary parts of $k_\perp$ calculated from the linear dispersion relation. The circles and lozenges are the real and imaginary parts of $k_\perp$, obtained from the simulation. The arrow in the figure indicates the position of the cyclotron subharmonic resonance: $\delta\omega_d = \frac{3}{2}\Omega_H - \omega + k_\parallel v_z = 0$.

values calculated from the linear dispersion relation which is shown as a solid curve. The imaginary parts of $k_\perp$ are approximately estimated and are shown in Fig. 1(c) as lozenges, indicating a significant absorption region near $\omega = \frac{3}{2}\Omega_H$. The linear theory, of course, predicts no damping here.

In Fig. 2(a), we show the spatial energy-deposition profile from $t = 32T$ to $60T$ ($T = 2\pi/\omega$), during which the wave propagation is in steady state. It is clear that the direct energy deposition to ions assumes the maximum value near the position at $x \cong 100$ where $\omega = \frac{3}{2}\Omega_H$.

In order to understand this result, we examine the motion of ions under the combined influence of the electrostatic wave $\phi_0 \cos(k_\perp x + k_\parallel z - \omega t)$ and an axial magnetic field with cyclotron frequency Ω. We assume $k_\perp >> k_\parallel$ and a constant velocity in z direction, i.e., $z = v_{z0}t$. When we select the appropriate spatial and time origins, the equations of motion are given without loss of generality as

$$\ddot{x} + \Omega^2 x = (q/m) k_\perp \phi_0 \sin(k_\perp x - \omega_d t), \qquad (1)$$

where $\omega_d = \omega - k_\parallel v_{z0}$.

If we perform the canonical transformations[4,5] of the Hamiltonian representing the motion described by Eq. (1), the Hamiltonian H can be separated into two parts: $H = H_0 + H_1$, the time-independent part H_0, and the time-dependent part H_1 with variables $\xi = p/s \arctan(\Omega x/\dot{x}) - \omega_d t$, $b = 0.5\Omega s/p (r/k_\perp)^2 = 0.5\Omega s/p\rho^2 = 0.5\Omega s/p (x^2 + \dot{x}^2/\Omega^2)$:

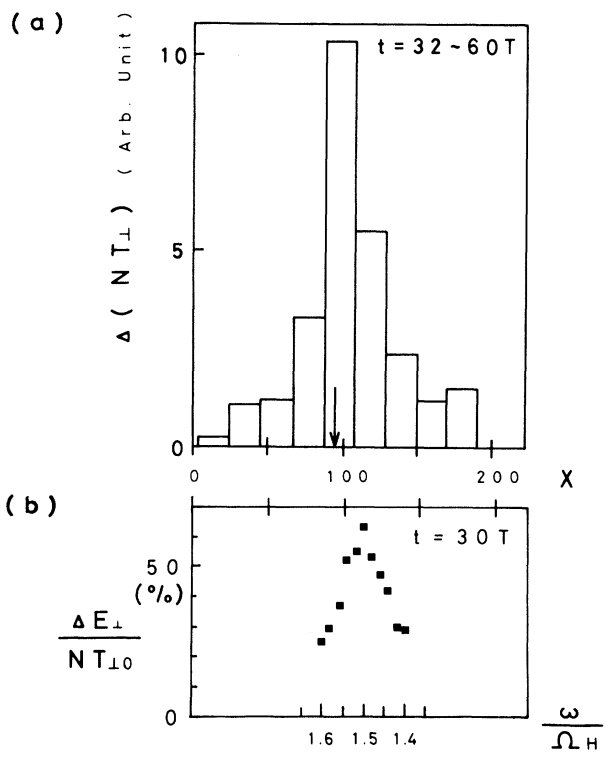

FIG. 2. The energy increase of ions. The arrow means the same as in Fig. 1(b). (a) The spatial profiles of the energy deposition to H in the simulation; (b) the energy increment in the single-particle simulation.

$$H_0(b, \xi) = \delta\omega_d b + q\phi_0 B_{s,p}[r(b)]\cos\xi, \qquad (2)$$

$$H_1(b, \xi, t) = q\phi_0 \sum_{\substack{n=-\infty \\ n \neq p}}^{\infty} B_{s,n}[r(b)]\cos\left[\frac{n}{p}\xi + \left(\frac{n}{p} - 1\right)\omega_d t\right], \qquad (3)$$

$$B_{s,n}(r) = \int_0^{2\pi} \cos(r \sin s\theta - n\theta)\, d\theta. \qquad (4)$$

where $\delta\omega_d = p\Omega/s - \omega + k_\parallel v_{z0}$, and we assume that s and p are integers which satisfy the condition that $s\Omega$ is close enough to $p\omega$.

Because $B_{s,p} \equiv 0$ for $s = 2$ and $p = 3$, however, the separation of H into $H_0 + H_1$ becomes meaningless for this case. In other words, the system can be considered to become degenerate. For the case of the finite wave amplitude, however, we must consider the first-order effects on the perturbed orbit due to the wave. Approximating the right-hand side of Eq. (1) by $q/mk_\perp\phi_0 \sin(-\omega_d t)$, we can easily obtain the perturbed orbit. Using the perturbation method, we can resolve the degeneracy and obtain a time-averaged orbit, following Ref. 5. For simplicity, we assume $s = 2$ and $p = 3$, and $\delta\omega_d = 0$. Expressing the time-averaging values for the short time ($\sim 1/\Omega$) by angled brackets $\langle\ \rangle$, we get

$$\langle\dot{r}\rangle = \alpha(p/s)\Omega(1/\langle r\rangle) C_{2,3}(\langle r\rangle)\sin\langle\xi\rangle, \qquad (5)$$

$$\langle\dot{\xi}\rangle = \alpha(p/s)\Omega(1/\langle r\rangle) C'_{2,3}(\langle r\rangle)\cos\langle\xi\rangle, \qquad (6)$$

$$C_{2,3}(r) = \int_0^{2\pi} \cos\{[r + \alpha\cos(\theta + \theta_0) + 0.2\alpha\cos(5\theta - \theta_0)]\sin 2\theta - 3\theta\}\, d\theta, \qquad (7)$$

where $\alpha = (E_\perp/B)/(\Omega/k_\perp) = qk_\perp^2\phi_0/(m\Omega^2)$, θ_0 is a phase between the wave and the cyclotron motion, and the prime denotes the derivative with respect to $\langle r\rangle$.

We have examined Eqs. (5)–(7) numerically and found that these approximations are useful to explain the qualitative behavior of the particle orbits and to predict both the trapping width and the bounce frequency with a good accuracy.

Although the trapping is concluded by Karney[6] not to occur in the case of $s=3$, we confirmed numerically the presence of the resonant acceleration near the one-third harmonics $s=3$, $\omega/\Omega \cong \frac{4}{3}$. Therefore, the same mechanism for s other than 2 can exist. We therefore believe that there exist some differences between the mechanism considered in Ref. 6 for $\omega >> \Omega_i$ and that considered here.

As a supplementary step to confirm the theory and to relate it to the self-consistent simulation results, we have performed the so-called single-particle simulation following Ref. 5. We have numerically calculated the exact equations of motions of many particles ($N=5000$) in the presence of a magnetic field and a monochromatic wave with the fixed wave amplitude, ω, and k including ∇B effects. The ∇B effects were found to contribute only several percent enhancement of the energy increment in the situation given in the simulation and may be neglected. A Maxwellian velocity distribution is assumed initially.

We adopted the parameter values $\alpha=0.31$, $k_\perp/k_\parallel=15$, and $k_\parallel v_{Ti0}/\Omega=0.05$, which are the averages of the measurement values at the position of interest ($x=66$–128) in the simulation. The normalized frequency ω/Ω is scanned from 1.6 to 1.4 corresponding to the positions from $x=86$ to 140 in the self-consistent simulation. The perpendicular energy increase per particle, $\Delta E_\perp/NT_{\perp 0}$, is shown in Fig. 2(b) for comparison. We can see the factor of ~ 3 enhancement at $\omega/\Omega=1.5$ compared with the values at the both sides ($\omega/\Omega=1.6$ and $\omega/\Omega=1.4$). In Figs. 3(a) and 3(b), we show the observed perpendicular energy distributions obtained from the self-consistent simulation and the single-particle simulation, respectively. In Fig. 4, the phase-space plot in $(v_\perp^2, v_\parallel)$ is shown for $\omega/\Omega=1.46$, which is a typical example. In this phase-space plot, the particles with v_z satisfying $\delta\omega_d/\Omega \sim 0$ are seen to be accelerated selectively. This confirms the particle trapping given by Eqs. (5) and (6).

The resonance around $\omega/\Omega=\frac{4}{3}$ is not observed in the self-consistent simulation. However, this resonance should also exist, although it is too weak to be observed for the parameters given in the simulation (a factor $\frac{1}{10}$ or weaker compared with the case of $s=2$: $\omega/\Omega=\frac{3}{2}$). We studied the general trend of this acceleration by using the single-particle simulations. We have observed that a significant trapping of the particles was observed when the values of $k_\perp v_{Ti0}/\Omega$ and the normalized wave amplitude α were doubled.

We have also run the particle-simulation code for a two-ion-species plasma where deuterium ions (D) are added. In this case, the resonant absorption at $3\Omega_D$ occurs along with the $\frac{3}{2}\Omega_H$ absorption without introducing significant change in the physics of the $\frac{3}{2}\Omega_H$ absorption. The resonant $3\Omega_D$ absorption becomes comparable when the deuterium concentration is increased to $\sim 20\%$. Although in the simulation only 25% of the incident wave power is absorbed by the $\frac{3}{2}\Omega_H$ process, in practice this absorption process can be very important. To scale this simulation result to an actual experimental situ-

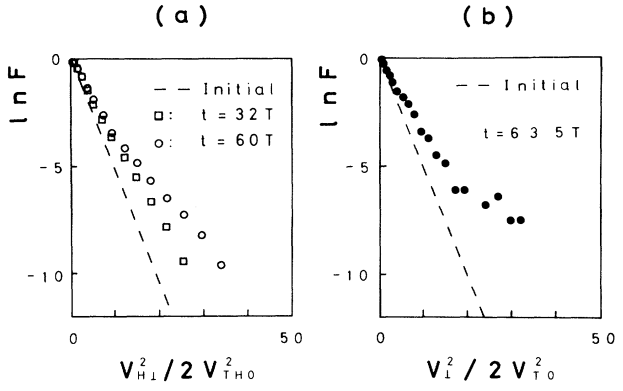

FIG. 3. The observed velocity distribution functions, $\ln f$ vs $v_\perp^2$: (a) for H in the simulation; (b) for the particles in the single-particle simulation.

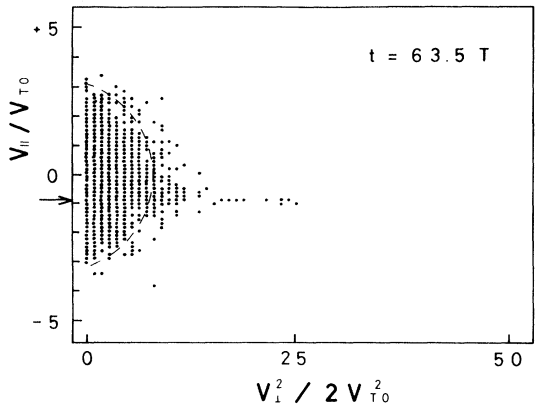

FIG. 4. The phase-space plot in $(v_\perp^2, v_\parallel)$ in the single-particle simulation ($\omega/\Omega=1.46$). The arrow indicates $v_\parallel$ which satisfies $\delta\omega_d=0$. The broken line indicates the boundary of the initial distribution.

ation, one important quantity is $\mathrm{Im}k_\perp R$ where R is the magnetic-field-gradient scale length, typically equal to the torus major radius. In the simulation, the system size is kept artifically small because of the computational restrictions. Since for ion Bernstein waves $\mathrm{Im}k_\perp \propto \mathrm{Re}k_\perp \propto \rho_H^{-1}$, the quantity of interest is R/ρ_H. In a typical tokamak experiment, this quantity is $\sim 10^3$ whereas in the simulation, this number is $\sim 10^2$. Thus an order-of-magnitude enhancement in R/ρ_H would suggest near-complete absorption of the incident ion Bernstein wave by the $\frac{3}{2}\Omega_H$ resonance in the actual experimental situation.[2]

It is interesting to note that in both the experiments (see Refs. 1 and 2) the significant changes in ΔT_i vs input power take place at the critical power levels, whose normalized wave amplitudes α are slightly larger than 0.3, which is in the range of α used in the simulation.

In conclusion, we have investigated the ion Bernstein wave heating by the self-consistent particle simulation code. The resonant feature of the energy deposition around the $\omega = \frac{3}{2}\Omega_H$ layer is shown to be the result of the ion acceleration efficiency enhancement due to a particle trapping by the finite-Larmor-radius cyclotron subharmonic wave. Since this mechanism can directly heat the bulk ion distribution of the majority ion species, it should be beneficial for heating fusion plasmas.

We thank Dr. A. Fukuyama, Dr. C. F. F. Karney, and Dr. H. Matsumoto at the Japan Atomic Energy Research Institute for useful discussions and comments. This work has been partially supported by an MOE grant in aid.

[1]M. Ono *et al.*, Phys. Rev. Lett. **52**, 37 (1984).

[2]M. Ono *et al.*, Institute of Plasma Physics, Nagoya University, Report No. IPPJ-662, 1984 (to be published).

[3]N. Nakajima, H. Abe, and R. Itatani, Phys. Fluids **25**, 2234 (1982).

[4]A. V. Timofeev, Nucl. Fusion **14**, 165 (1974).

[5]H. Abe, H. Momota, R. Itatani, and A. Fukuyama, Phys. Fluids **23**, 2417 (1980).

[6]C. F. F. Karney, Phys. Fluids **22**, 2188 (1979).